HHS Public Access

Author manuscript

J Immunol. Author manuscript; available in PMC 2017 July 15.

Published in final edited form as:

J Immunol. 2016 July 15; 197(2): 458–469. doi:10.4049/jimmunol.1502283.

The lupus susceptibility gene *Pbx1* regulates the balance between follicular helper T cell and regulatory T cell differentiation

Seung-Chul Choi, **Tarun E. Hutchinson**, **Anton A. Titov**, **Howard R. Seay**, **Shiwu Li**, **Todd M. Brusko**, **Byron P. Croker**, **Shahram Salek-Ardakani**, and **Laurence Morel**[*,1]

Department of Pathology, Immunology, and Laboratory Medicine, University of Florida, Gainesville, FL 32610, USA

Abstract

Pbx1 controls chromatin accessibility to a large number of genes and is entirely conserved between mice and humans. The *Pbx1-d* dominant negative isoform is more frequent in the $CD4^+$ T cells from lupus patients than from healthy controls. *Pbx1-d* is associated with the production of autoreactive T cells in mice carrying the *Sle1a1* lupus susceptibility locus. Transgenic expression of *Pbx1-d* in $CD4^+$ T cells reproduced the phenotypes of *Sle1a1* mice, with increased inflammatory functions of $CD4^+$ T cells and impaired regulatory T cell homeostasis. *Pbx1-d* Tg also expanded the number of follicular helper T cells in a cell-intrinsic and antigen-specific manner that was enhanced in recall responses, and resulted in T_H1-biased antibodies. Moreover, *Pbx1-d* Tg $CD4^+$ T cells upregulated the expression of miR-10a, miR-21 and miR-155, which have been implicated in Treg and T_{FH} cell homeostasis. Our results suggest that *Pbx1-d* impacts lupus development by regulating effector T cell differentiation and promoting T_{FH} cells at the expense of Treg cells. In addition, our results identify *Pbx1* as a novel regulator of $CD4^+$ T cell effector function.

Keywords

Pbx1; regulatory T cells; follicular helper T cells; SLE; microRNA

Introduction

The NZM2410 murine strain was derived from the classical (NZB x NZW) F1 model of systemic lupus erythematosus (SLE), which is an autoimmune disease characterized by the production of autoantibodies (autoAbs) to nuclear antigens (Ag), immune activation, and

[*]Address correspondence and reprint requests to Dr. Laurence Morel, Department of Pathology, Immunology and Laboratory Medicine, University of Florida, Gainesville, FL 32610-0275, USA. Tel: (352) 392-3790, Fax: (352) 392-3053. morel@ufl.edu.

[1]This study was supported by NIH grants R01 AI045050 to LM and AI087734 to SSH.

Author Contributions

Author contribution: SCC, TMB, S-SA and LM designed experiments; SCC, TEH, AAT, HRS, SL, BPC carried out experiments; SCC, TEH, AAT, and LM analyzed data; and SCC, S-SA and LM wrote the paper.

Conflict of Interest

The authors declare no conflict of interest.

immune-complex mediated inflammation in various tissues. We have mapped three major NZM2410 lupus susceptibility loci, and generated three congenic strains, B6.NZM*Sle1*, -*Sle2*, and -*Sle3*, each carrying the corresponding NZM2410-derived genomic interval on the C57BL/6J (B6) genome (1, 2). Analysis of immunological properties of each congenic strain in comparison to B6 showed that *Sle1* and *Sle3* increase T cell activation and effector functions, and that *Sle1* and *Sle2* promote the development of autoreactive B cells and B cell hyperactivity (3).

Sle1 on telomeric chromosome 1 was the locus with the strongest linkage to lupus nephritis, and its expression is required for the development of systemic autoimmunity and pathogenesis in the NZM2410 model (4, 5). *Sle1* expression results in the production of autoAbs specific for chromatin (6) through intrinsic defects in B and $CD4^+$ T cells (7). Three *Sle1* independent sub-loci, *Sle1a*, *Sle1b*, and *Sle1c*, contribute to autoimmune phenotypes (8). *Sle1a* and *Sle1c* induce the production of activated autoreactive T cells and decrease the number and function of $Foxp3^+$ regulatory $CD4^+$ (Treg) cells (9–11). *Sle1b* is associated with extensive polymorphisms between two divergent haplotypes of the SLAM family, and it regulates B cell (12) as well as T cell (13) tolerance. *Sle1a* has been mapped to two interacting loci, *Sle1a1* and *Sle1a2* (14). *Sle1a1* contains only one functional known gene, pre-B cell leukemia homeobox 1 (*Pbx1*), and the lupus-associated allele corresponds to the increased expression of a novel splice isoform, *Pbx1-d,* in $CD4^+$ T cells (15). *Pbx1*, a member of the three-amino-acid-loop-extension (TALE) class of homeodomain proteins, is a transcriptional factor that regulates chromatin access of multimeric complexes that include Hox factors, as well as myeloid ecotropic viral integration site (*Meis*) and Pbx-regulating protein-1 (*Prep-1*), two other TALE proteins that regulate chromatin remodeling and coactivator access (16). The interactions of Pbx-Meis/Prep-1 complexes with both Hox and non-Hox factors ultimately contribute to either gene activation or repression (17). *Pbx1-d* lacks exons 6 and 7 corresponding to the DNA binding domain and the Hox binding domain, respectively, which confers this splice isoform a dominant-negative function (18).

Sle1a1 expands the number of activated and autoreactive $CD4^+$ T cells, and reduces the number of peripheral Treg (pTreg) cells in a $CD4^+$ T cell intrinsic manner (15). These T cell phenotypes were not sufficient however to induce a robust production of autoAbs in B6.*Sle1a1* mice, which requires the expression of *Sle1* in B cells (14). In addition, *Pbx1-d* expression is associated with abnormal responses to TGF-β and retinoic acid (RA) in both murine and human T cells (19). *Pbx1* expression is necessary for B cell development (20), but its function in T cells is unknown. The goal of this study was to directly address the role of *Pbx1-d* over-expression in $CD4^+$ T cells. We showed that transgenic B6 mice that overexpress *Pbx1-d* in their $CD4^+$ T cells (*Pbx1-d* Tg mice) reproduce the phenotypes of B6.*Sle1a1* mice, with increased inflammatory functions of $CD4^+$ T cells and impaired Treg cells homeostasis. In addition, *Pbx1-d* Tg mice showed a follicular helper T (T_{FH}) cell population that expanded in an Ag-specific and T-cell intrinsic manner, with an enhanced capacity to locate in B cell follicles and to promote affinity maturation of T_H1-associated Ab isotypes. These results suggest that *Pbx1* regulates the balance between pTreg and T_{FH} cell maintenance or differentiation, and that *Pbx1-d* contributes to autoimmunity by tilting the balance in favor on T_{FH} over Treg cells.

Materials and Methods

Mice

B6.CD4-*Pbx1-d* Tg (*Pbx1-d* Tg) mice were generated at the University of Florida transgenic core using a bicistronic *Pbx1-d*/GFP cDNA controlled by the CD4 promoter (Sup. Fig. 1A) in a C57BL/6J background. Four Tg lines were obtained, with a Tg copy number of 8–13 in the A886, C855 and A872 lines, and 30 in the C861 line (Sup. Fig. 1B). GFP protein expression was not achieved in any of the lines. The following primers were used to detect *Pbx1-d* Tg are: Forward (spanning exons 5 and 8): ATCACAGTCTCCCAGGTGGA, and Reverse (in exon 9): ATCCTGCCAACCTCCATTAG. *Pbx1-d* expression was restricted to $CD4^+$ T cells (Sup. Fig. 1B and C). Primer and Taqman probe sequences used to measure *Pbx1-d* message expression have been described (21). Mice from all four lines were healthy at least up to one year of age. Results reported in this study were obtained with mice from the first three lines, without any difference observed between lines. C861 mice were not included due to poor breeding performance. Initial characterization was performed with Tg-negative littermates, which presented phenotypes identical to that of B6 controls. No difference was observed between hemizygous and homozygous lines, indicating that within the observed range, the Tg copy number was not critical for the phenotypes. The results reported in this study were obtained with homozygous mice. B6, B6.SJL-*Ptprc*^{a}*Pep3*^{b}/BoyJ (B6.Ly5^a), B6.Cg-Tg(TcraTcrb)425Cbn/J (B6.OT-II) and B6.129S7-*Rag1*^{tm1Mom}/J (B6.*Rag-1*$^{-/-}$) mice were originally obtained from the Jackson Laboratory. B6.Thy1^a.OT-II mice were graciously provided by Dr. Stephen Schoenberger. The B6.*Sle1a.1*$^{NZW/NZW}$ (B6.*Sle1a1*) and B6.NZM-*Sle1*$^{NZM2410/Aeg}$*Sle2*$^{NZM2410/Aeg}$*Sle3*$^{NZM2410/Aeg}$/LmoJ (B6.TC) congenic mice have been previously described (5, 14). B6.Foxp3-enhanced GFP (B6.*Foxp*^{egfp}) mice (22) were kindly provided by Dr. V. J. Kuchroo. *Pbx1-d* Tg.*Foxp3*^{egfp} mice were bred from the A886 line and *Pbx1-d* Tg.OT-II were bred from the C855 line. All mice were bred and maintained at the University of Florida in specific pathogen-free conditions. Only female mice, except for the colitis experiment, were used in this study under a protocol approved by the Institutional Animal Care and Use Committee of the University of Florida.

T cell polarization

In vitro induced Treg (iT_{reg}) cells were differentiated as previously described (15). Briefly, $CD4^+CD25^-$ cells were negatively selected from B6 or *Pbx1-d* Tg splenocytes using the $CD4^+CD25^+$ Treg isolation kit (Miltenyi Biotech), and then 5×10^5 cells were stimulated with mouse T-activator CD3/CD28 beads (Life Technologies) at the concentration of 1×10^6 beads/mL in the presence of 100 U IL-2, 20 ng/ml TGF-β (Pepro Tech), and 0–5 nM all-trans retinoic acid (RA) for 5 d. T_H1 and T_H17 polarization was performed as previously described (23).

Flow cytometry

Single-cell suspensions were prepared using standard procedures from spleen, thymus, and mesenteric lymph node (mLN). After red blood cell lysis, cells were blocked with anti-CD16/32 Ab (2.4G2), and stained in FACS staining buffer (2.5% FBS, 0.05% sodium azide in PBS). Fluorochrome-conjugated Abs used were to B220 (RA3-6B2), BCL6 (K112-91),

CD4 (RAM4-5), CD8 (53-6.7), CD25 (PC61.5), CD44 (IM7), CD45.1 (A20), CD45.2 (104), CD62L (MEL-14), CD69 (H1.2F3), CD95 (Jo2), CD90.1 (HIS51), CD90.2 (53-2.1), Foxp3 (FJK-16s), Ly-77 (GL7), Neuropilin-1 (761705), PD-1 (RMP1-30), IFN-γ (XMG1.2), IL-2 (JES6-5H4), IL-17a (eBio17B7), and IL-21 (FFA21) purchased from BD Biosciences, eBioscience, BioLegend, and R&D Systems. Follicular T cells were stained as previously described (55) in a three-step process using purified CXCR5 (2G8) followed by biotinylated anti-rat IgG (Jackson ImmunoResearch), then PerCP5.5-labeled streptavidin in FACS staining buffer on ice. Dead cells were excluded with fixable viability dye (eFluor780; eBioscience). Data were collected on LSRFortessa (BD Biosciences) and analyzed with FlowJo software (Tree Star).

Mixed bone marrow (BM) chimera and adoptive cell transfers

Chimeras were prepared as previously described (9) with the following modifications. 8–10 week-old (B6 x B6.Ly5^a)F1 recipient mice were lethally irradiated with two doses of 452 rad (4 h apart) using an X-RAD 320 irradiator (Precision X-Ray). Donor BM cells were depleted of mature T cells using CD5 MicroBeads (Miltenyi Biotech). Mixed 1:1 BM cells (1×10^7 cells) were given to the recipient mice by tail-vein injection. Treg cells were analyzed in chimeric mice 8 weeks later. For T-dependent (TD) immune responses, chimeric mice were immunized with 100 μg of NP_{23}-KLH (Biosearch Tech.) in alum 8 weeks after BM cell transplantation, and T_{FH} cells were analyzed 1 week after immunization. CD4$^+$ T cells from *Pbx1-d* Tg.OT-II, B6.*Sle1a1*.OT-II and B6.OT-II mice were purified by negative selection using MACS MicroBeads, then 0.5×10^6 cells were tail-vein injected into B6.Ly5^a mice, followed by subcutaneous immunization with 50 μg NP_{16}-OVA in alum 4 h after cell transfer. For mixed adoptive transfer, CD4$^+$ T cells from *Pbx1-d* Tg.OT-II or B6.*Sle1a1*.OT-II and B6.Thy1^a.OT-II mice were mixed at 1:1 ratio, and 1×10^6 cells were injected into (B6 x B6.Thy1^a)F1 recipient mice prior to immunization with NP_{16}-OVA.

To assess the function of effector T (T_{Eff}) cells *in vivo*, 4×10^5 purified CD4$^+$CD25$^-$$T_{Eff}$ cells from 2 month-old *Pbx1-d* Tg and B6 mice were tail-vein injected into B6.*Rag-1*$^{-/-}$mice. The function of Treg cells was evaluated in co-injections of 1×10^5 CD4$^+$CD25$^+$ Treg cells from either *Pbx1-d* Tg or B6 mice along with 4×10^5 CD4$^+$CD25$^-$B6 T_{Eff} cells. Recipient mice were monitored for clinical signs of colitis for up to 8 weeks and body weight was monitored weekly. The recipient mice that lost more than 15% body weight or showed overt clinical signs of disease were sacrificed. Colon histology was ranked blindly in a semi-quantitative fashion as previously described (9).

Immunohistochemistry

To stain splenic germinal centers (GCs) in B6.Ly5^a mice that received *Pbx1-d* Tg.OT-II or B6.OT-II CD4$^+$ T cells, 7 μm thick OCT-embedded cryosections were prepared on super-frost glass, washed with PBS, fixed with 4% paraformaldehyde for 15 min at 4°C, and subsequently permeabilized with 0.1% Triton X-100 for 5 min at 4°C. The sections were washed with cold PBS and incubated overnight in the dark at 4°C with anti-CD45.2 conjugated to PE, anti-GL7 conjugated to AF488, and anti-IgD conjugated to APC (all from eBioscience). Sections were washed three times with cold PBS, mounted with cytoseal, and covered with glass coverslip. The stained sections were analyzed using an EVOS FL digital

inverted fluorescence microscope (Fisher Scientific, Waltham, MA), images were captured by ×10, ×20, and ×40 objectives, keeping all of the conditions of microscope and settings of software identical for all treatments and controls.

Immunization and Ab measurements

For TD responses, 8–10 wk-old mice were immunized intra-peritoneally with 100 μg NP_{23}KLH in alum, and boosted at week 2 and 6. Serum samples were collected 1, 3, 5, and 7 weeks after the first immunization. NP-specific Abs were measured by ELISA using NP_4- or NP_{25}-BSA (Biosearch Tech.) coated plates, followed by incubation with 1:1000 diluted serum samples and developed with alkaline phosphatase-conjugated goat anti-mouse IgG1, IgG2a, IgG2c, IgG3, or IgM (Southern Biotech). All samples were run in duplicate. Anti-dsDNA and anti-chromatin IgG were measured as previously described (6) in sera diluted 1:100, and relative units were standardized using serial dilutions of a positive serum from B6.TC mice, setting the 1:100 dilution reactivity to 100 U. Serum anti-nuclear Ab (ANA) were measured by applying 1:40 diluted sera to fixed Hep-2 cells (Inova) and revealed with anti-mouse IgG-FITC (Invitrogen).

miRNA analysis

Splenic $CD4^+$ T cells from *Pbx1-d* Tg.*Foxp3*^{egfp}, B6.*Sle1a1.Foxp3*^{egfp}, and B6.*Foxp3*^{egfp} mice were first enriched by negative selection using MACS MicroBeads, then GFP^+ and GFP^-cells were sorted with a FACSAria cytometer with a purity ≥ 95%. miRNAs were isolated and reverse transcribed using Life Technologies reagents. Quantification of miRNAs expression was performed using TaqMan MicroRNA assays (Life Technologies) using the Applied Biosystems StepOne™ real-time PCR machine. U6 snRNA was used as internal control. Comparisons were made using the $2^{-\Delta\Delta Ct}$ method and values were normalized to the B6 average values.

Luciferase assay

Putative human PBX1 binding sites in the ~ 2 Kb flanking miR-10a, miR-21 and miR-155 precursors were identified using Jaspar3 (set for 75% accuracy). We generated luciferase reporter constructs containing the 798-bp, 1071-bp and 850-bp region upstream of miR-10a, miR-21 and miR-155, respectively (Fig. 8A) cloned into the pGL4.25 Luciferase vector (Promega). PBX1-b or PBX1-d expression plasmids were generated by inserting cDNAs (15) into the pHAGE-CMV-MCS-IzsGreen plasmid. The luciferase reporter constructs and the pGL3-basic plasmid were then each co-transfected with either PBX1-b or PBX1-d expression plasmid into HEK293T cells. Cells were harvested after 48 h. After lysis with the Passive Lysis Buffer (Promega), luciferase activity was measured using a dual luciferase reporter assay system (Promega) according to the manufacturer's instructions with a Lumat LB 9507 luminometer (Berthold Technologies).

Statistical analysis

Differences between groups were evaluated by two-tailed statistics: unpaired *t* tests or Mann-Whitney *U* tests depending on whether the data was normally distributed, paired *t* tests for mixed BM-chimeras, χ^2 tests to compare distributions, and two-way ANOVA tests

for time-course experiments. Unless specified, graphs show means and standard deviations of the mean. *$P < 0.05$, **$P < 0.01$, and ***$P < 0.001$.

Results

Pbx1-d Tg mice replicated the phenotypes of B6.*Sle1a1* mice

To address whether the overexpression of *Pbx1-d* in $CD4^+$ T cells was sufficient to induce their activation and loss of tolerance, we generated *Pbx1-d* Tg mice that express *Pbx1-d* driven by the *Cd4* promoter (Supl. Fig. 1). *Pbx1-d* Tg overexpression in $CD4^+$ T cells resulted in the production of serum ANA with the characteristic homogenous nuclear staining pattern (Fig. 1A) as well as anti-dsDNA and anti-chromatin IgG in 7 to 12 month old mice (Fig. 1B and C). A similar nuclear staining pattern was observed in the serum of B6.*Sle1a1* mice, although with a lower intensity, which is consistent with a low level of anti-dsDNA and anti-chromatin IgG (Fig. 1B and C), as we have previously reported for this strain (14, 15). This suggested that *Pbx1-d* overexpression results in the production of autoreactive $CD4^+$ T cells that are sufficient to induce humoral autoimmunity against nuclear Ag. B6.*Sle1a1* mice were characterized by the expansion of $CD44^+CD62L^-$effector memory T (T_{EM}) cells relative to $CD44^-CD62L^+$ naïve T (T_N) cells (15). Aged *Pbx1-d* Tg mice also presented a skewed T_N/T_{EM} ratio (Fig. 1D). We examined the consequence of *Pbx1-d* overexpression in $CD4^+CD25^-T_{Eff}$ cells *in vivo* with the experimental colitis model that we have used with B6.*Sle1a1* T cells (9). B6.*Rag1*$^{-/-}$ mice that received *Pbx1-d* Tg T cells showed a greater body weight loss and a Eff more severe colitis than the mice that received B6 T_{Eff} cells (Fig. 1E–F). These results suggest that *Pbx1-d* expression is sufficient to induce an intrinsic activation in $CD4^+$ T cells. However, we observed a similar ability of *Pbx1-d* Tg or B6 $CD4^+CD25^+$ T cells to suppress B6 T_{Eff} cells in the same colitis model (data not shown), suggesting that *Pbx1-d* Tg Treg *in vivo* functions were less affected than that of B6.*Sle1a1* Treg cells (14).

Pbx1-d overexpression impaired Treg cell homeostasis

To assess the role of *Pbx1-d* in Treg cells as compared to conventional $CD4^+$ T cells, we bred the *EGFP-Foxp3* reporter construct to both B6.*Sle1a1* and *Pbx1-d* Tg mice. *Pbx1-d* expression in *Pbx1-d* Tg $CD4^+$ T cells was ~ 10,000 folds higher than in B6 T cells, and was similar in $Foxp3^+$ and $Foxp3^-$ cells (Fig. 2A–B). *Pbx1-d* expression in the *Pbx1-d* Tg T cells was also much higher (~100 folds) than in B6.*Sle1a1* mice in either $Foxp3^+$ or $Foxp3^-$T cells (Fig 2A–B). As previously reported for B6.*Sle1a1* mice (14, 15), the frequency of $CD4^+Foxp3^+$ Treg cells was reduced in *Pbx1-d* Tg mice with the largest difference in the mLN (Fig. 2C). In addition, *in vitro* iTreg cell polarization by TGF-β and RA was reduced in *Pbx1-d* Tg $CD4^+CD25^-$T cells as compared to B6 cells (Fig. 2D). These results indicate that, as *Sle1a1*, *Pbx1-d* overexpression in $CD4^+$ T cells impairs iTreg differentiation by interfering with the response to RA in the presence of TGF-β.

To further evaluate the impact of *Pbx1-d* on Treg differentiation, we reconstituted lethally irradiated (B6 x B6.Ly5^a)F1 mice with T cell-depleted BM cells mixed from *Pbx1-d* Tg and B6.Ly5^a mice (Fig. 2E). *Pbx1-d* Tg BM yielded to a decreased percentage of $CD4^+Foxp3^+Nrp\text{-}1^-$pTreg cells as compared to the B6.Ly5^a BM in the thymus of the

recipient mice, whereas the proportion of $CD4^+Foxp3^+Nrp\text{-}1^+$ thymic Treg (tTreg) cells was similar between the two genotypes (Fig. 2F–H). In these conditions, however, the proportions of Treg cells in the peripheral organs of recipient mice were similar for BM-derived cells of either genotypes (data not shown), possibly due to the relatively short time between BM transfer and phenotype readout. Together these data indicate that *Pbx1-d* Tg overexpression in $CD4^+$ T cells impairs the induction or maintenance of pTreg cells in a cell-intrinsic manner.

Pbx1-d Tg overexpression in $CD4^+$ T cells expanded the number of T_{FH} cells

Since *Pbx1-d* overexpressing $CD4^+$ T cells showed an activated phenotype (Fig. 1D), we next examined their cytokine production. *Ex vivo Pbx1-d* Tg $CD4^+$ T cells showed a significantly increased IL-21 expression (Sup. Fig. 2A–B) as compared to B6, but there was no difference for the level of IL-2, IL-17A or IFN-γ production (Sup. Fig. 2A, C–E), or the frequency of $IL\text{-}17A^+$ or $IFN\text{-}\gamma^+$ $CD4^+$ T cells (data not shown). Under *in vitro* T_H1 polarization conditions, a small but significant difference was observed with *Pbx1-d* Tg $CD4^+$ T cells producing more IFN-γ than B6 cells, while there was no difference for IL-17A (Sup. Fig. 2F and G). These results prompted us to investigate T_{FH} cell differentiation in *Pbx1-d* Tg mice. T_{FH} cells secrete high levels of IL-21, and IL-21 signaling up-regulates *Bcl6* expression, which is required for the development of T_{FH} cells and germinal center (GC) formation (24–27). At steady state, young (6–8 weeks) *Pbx1-d* Tg and B6.*Sle1a1* mice showed an increased cellularity in the mLN, where the numbers and percentages of GC B cells were also increased as compared to B6 (Fig. 3A–C). The percentages and absolute numbers of $CD4^+PD1^+CXCR5^+Bcl6^+Foxp3^-T_{FH}$ cells were significantly higher in the mLN from *Pbx1-d* Tg mice, but not in their spleen (Fig. 3D–F). A similar trend was observed for B6.*Sle1a1* T_{FH} cells. On the other hand, the number of $CD4^+PD1^+CXCR5^+Bcl6^+Foxp3^+$ follicular regulatory T (T_{FR}) cells was significantly reduced in the spleen of *Pbx1-d* Tg mice (Fig. 3F). We next tested the differentiation of T_{FH} and T_{FR} cells 7 d after administrating a TD Ag into chimeric mice reconstituted with a 1:1 mix of *Pbx1-d* Tg and B6 BM (Fig. 3G). The number and percentage of both *Pbx1-d* Tg-derived T_{FH} and T_{FR} cells were significantly increased as compared to B6-derived cells (Fig. 3H and I). The discrepancy between the unchanged frequency or a decreased number of *Pbx1-d* Tg T_{FR} cells in unmanipulated mice (Fig. 3E and F) on one hand and the increased number and frequency of *Pbx1-d* Tg-derived T_{FR} cells in chimeric mice (Fig. 3H and I) on the other hand is likely due to homeostatic expansion that favors all Bcl6-expressing *Pbx1-d* Tg-derived T cells. The numbers of B6 and *Pbx1-d* Tg-derived total $CD4^+$ T cells were similar before immunization, indicating an Ag-driven enhancement of T_{FH} cell differentiation by *Pbx1-d* overexpression. These steady-state and immunization results are consistent with *Pbx1-d* overexpression in $CD4^+$ T cells increasing T_{FH} cell differentiation in a cell-intrinsic manner.

Pbx1-d Tg overexpression enhanced Ag-specific T_{FH} cell differentiation and follicular localization

To track T_{FH} cells in an Ag-specific manner, *Pbx1-d* Tg mice were bred with B6.OT-II mice, which express an MHC class II-restricted T cell receptor specific for ovalbumin (OVA) (28). *Pbx1-d* Tg.OT-II or B6.OT-II $CD4^+$ T cells were transferred into B6.$Ly5^a$ mice, which were then immunized with NP-OVA. By d 5 after immunization, *Pbx1-d* Tg.OT-II and B6.OT-II

total $CD4^+$ T cells were expanded to a similar extent, and there was no difference for the recipient $CD45.1^+$ T cells (Fig. 4A). However, the $CD45.2^+$ *Pbx1-d* Tg.OT-II $CD4^+$ T cells contained a higher frequency and number of T_{FH} cells (Fig. 4B and C) than the B6.OT-II $CD4^+$ T cells. Either *Pbx1-d* Tg.OT-II or B6.OT-II transferred $CD4^+$ T cells produced very low numbers of T_{FR} cells (Fig. 4A). Homing of primed T_{FH} cells to B cell follicles is a critical step to generate GCs. The number of transferred *Pbx1-d* Tg.OT-II $CD4^+$ T cells within the B cell zone was significantly higher than the number of B6.OT-II $CD4^+$ T cells, whereas there was no difference in the number of transferred T cells in the T cell zone (Fig. 4D and E). In addition, CXCR5 and Bcl6 expression was significantly higher in the transferred *Pbx1-d* Tg.OT-II than the transferred B6.OT-II $CD4^+$ T cells (CXCR5: 483 ± 18.14 vs. 430.20 ± 10.14, $P < 0.001$; Bcl6: 507.20 ± 23.21 vs. 436.60 ± 13.86, $P < 0.05$). At d 7 after immunization, there was a similar frequency of *Pbx1-d* Tg.OT-II and B6.OT-II T_{FH} cells (Supplemental Fig. 3A), and a similar number of these cells in the spleen (Supplemental Fig. 3B), although the number of *Pbx1-d* Tg.OT-II T_{FH} cells was still higher in the mLN (Supplemental Fig. 3B). Interestingly, the number of total *Pbx1-d* Tg.OT-II T cells was increased in both spleen and mLN (Supplemental Fig. 3C). This expanded population was largely absent from the GC (Supplemental Fig. 3D), suggesting that they may correspond to extrafollicular helper T cells, a population that is expanded in lupus-prone mice (29).

We performed the same experiment with B6.*Sle1a1*.OT-II $CD4^+$ T cells, which generated a similar frequency and number of T_{FH} cells as well as a similar number of B6.*Sle1a1*.OT-II $CD4^+$ T cells located in the B cell follicles than B6.OT-II $CD4^+$ T cells 5 d after immunization (Fig. 4F–G). At d 7 after immunization, the number and frequency of T_{FH} cells were also similar between cells of *Sle1a1* or B6 origin (Supplemental Fig. 3E and F). The number of total *Sle1a1*.OT-II $CD4^+$ T cells was however higher in the spleen than B6.OT-II T cells and there was a trend in the mLN (Supplemental Fig. 3G). Therefore, these results suggest that a high level of *Pbx1-d* expression in $CD4^+$ T cells increased Ag-specific T_{FH} cell differentiation as well as early entry in B cell follicles, while the more modest increased expression of Pbx1-d in Sle1a1 $CD4^+$ T cells increased their Ag-specific expansion.

We then examined the effect of *Pbx1-d* overexpression on T_{FH} cell differentiation in a competitive setting by co-transferring B6.$Thy1^a$.OT-II and *Pbx1-d* Tg.OT-II (1:1) $CD4^+$ T cells into (B6 x B6.$Thy1^a$)F1 recipient mice. Five days after primary NP-OVA immunization (Fig. 5A), the percentage of total B6.$Thy1^a$.OT-II $CD4^+$ T cells was higher than that of *Pbx1-d*.OT-II Tg $CD4^+$ T cells in the spleen and mLN, and the same trend was observed for *Sle1a1*.OT-II $CD4^+$ T cells (Fig. 5B). A higher percentage of T_{FH} cells was only found with *Pbx1-d* Tg origin in the mLN (Fig. 5C). We next asked whether *Pbx1-d* overexpression influenced the recall Ag-response in the same model (Fig. 5A). In contrast to the primary response, the percentages of *Pbx1-d*.OT-II Tg and *Sle1a1*.OT-II total $CD4^+$ T cells (Fig. 5D) and T_{FH} cells (Fig 5E) were higher than that of corresponding cells of B6 origin in the spleen and mLN at 3 d after secondary immunization. Moreover, the relative expansion of the T_{FH} subset was significantly greater in cells from *Pbx1-d* Tg or *Sle1a1* origin as compared to cells from B6 origin in the recall as compared to the primary response (Fig. 5F). Finally, the percentage of *Pbx1-d* Tg activated (Fig. 5G–H) and $CD44^{hi}$ memory $CD4^+$

T cells (Fig 5I–J) was enhanced, which we did not observed during the primary response. Taken together, these results indicate that *Pbx1-d* overexpression conferred a cell-intrinsic competitive advantage during Ag-specific T_{FH} cell differentiation that was enhanced during recall responses.

Pbx1-d Tg mice responded to TD Ags with an increased T_H1-related Ig isotypes

To assess the effect of *Pbx1-d* overexpression on affinity maturation and class-switching, B6 and *Pbx1-d* Tg mice were boosted 2 and 6 weeks after primary immunization with NP-KLH. *Pbx1-d* Tg mice produced significantly more high and low affinity anti-NP-IgG3 and high-affinity anti-NP IgG2a and IgG2c than B6 mice (Fig. 6A–B). Moreover, the affinity of anti-NP IgG2a and IgG2c as measured by the NP_4/NP_{25} ratio was significantly increased in *Pbx1-d* Tg mice after boosting (Fig. 6C), suggesting that *Pbx1-d* overexpression increases affinity maturation of T_H1-associated antibodies.

Pbx1-d overexpression increased the expression of miR-10, miR-21 and miR-155 in $CD4^+$ T cells

Numerous studies have implicated microRNAs (miRNAs) in Treg and T_{FH} cell differentiation and functions (30). We have analyzed the effect of *Pbx1-d* overexpression on candidate miRNAs selected for their role in this process (miR-10a, -17, -19a, -19b, -20a, -21, -92, -155, -181a, and -181b) in Foxp3-GFP^+ and Foxp3-GFP^-CD4^+ T cells from young *Pbx1-d* Tg.*Foxp3*^{egfp}, B6.*Sle1a1.Foxp3*^{egfp}, and B6.*Foxp3*^{egfp} mice. miR-10a, miR-21 and miR-155 expression was 2–3 fold higher in either *Pbx1-d* Tg or B6.*Sle1a1* than in B6.Foxp3-GFP^+ Treg cells (Fig. 7A). The same result was obtained for *Pbx1-d* Tg Foxp3-GFP^-conventional $CD4^+$ T cells, while expression of miR-21 and miR-155 was more variable in B6.*Sle1a1* Foxp3-GFP^-CD4^+ T cells, although going in the same direction (Fig. 7B). The expression of miRNAs from the miR17~92 and miR181 families was significantly increased in Foxp3-GFP^+ Treg cells from B6.*Sle1a1* mice, but not in Treg cells from *Pbx1-d* Tg mice and there was no consistent difference between strains in Foxp3-GFP^-conventional T cells (Supplemental Table 1). These findings indicate that *Pbx1-d* affects the expression of specific miRNAs that have been associated with $CD4^+$ Treg and T_{FH} cell differentiation and function, either directly or indirectly.

To address whether the increased expression of miR-10a, miR-21 and miR-155 found in *Pbx1-d* Tg and B6.*Sle1a1* $CD4^+$ T cells was maintained in mice with clinical lupus phenotypes, we analyzed B6.*Sle1.Sle2.Sle3* (TC) mice, which carry the *Sle1a1* allele of *Pbx1* (5). TC mice present spontaneously expanded subsets of T_{FH} cells (Fig. 7C and D). miR-10a, miR-21 and miR-155 were expressed at a higher level in TC $CD4^+$ T cells starting at 2 months of age, before the mice produce autoAbs and show overt signs of autoimmune activation (Fig. 7E). These results suggest that the up-regulation of these three miRNAs driven by *Pbx1-d* overexpression in the Tg mice contributes to the autoimmune phenotype in lupus mice that express the Pbx1-d allele.

miR-21 expression is regulated by the PBX1/HOX9 complex in leukemia (31), suggesting that Pbx1 could directly regulate the transcription of miR-10a, miR-21 and miR-155. An *in silico* analysis identified several putative PBX1 binding sites for each of the three miRNAs

that are overexpressed in *Pbx1-d* Tg T cells. We co-transfected HEK293T cells with one of three luciferase constructs containing the upstream regulatory region for miR-10a, miR-21 or miR-155 that contained the most proximal putative PBX1 binding sites (Fig. 8A) and plasmids expressing either the normal allele PBX1-b or the lupus allele PBX1-d cDNA. As shown in Fig. 8B, PBX1-b and PBX1-d increased the transcription of each of the three miRNA, with higher levels obtained for PBX1-d than PBX1-b for miR-10a and miR-155. These data strongly support transcriptional regulation of miR-10a, miR-21 and miR-155 by PBX1.

Discussion

This study examined the role of *Pbx1-d* expression in $CD4^+$ T cells relative to the phenotypes induced by the *Sle1a1* lupus susceptibility locus. *Sle1a1* increases $CD4^+$ T cell effector functions and reduces the number and function of Treg cells, resulting in the production of autoreactive $CD4^+$ T cells (9, 11). *Pbx1-d* over expression in the $CD4^+$ T cells of B6 mice resulted in autoAb production and T cell activation as well as a decreased number of pTreg cells and a reduced iTreg differentiation *in vitro*. These results are fully consistent with *Pbx1-d* overexpression being responsible for *Sle1a1* $CD4^+$ T cell activation and impaired iTreg cell differentiation or maintenance (9). The most striking phenotype of *Pbx1-d* Tg mice was however the expansion of T_{FH} cells and associated TD immune responses. BM chimera and adoptive transfer studies showed that *Pbx1-d* overexpression resulted in a cell-intrinsic Ag-specific expansion of T_{FH} cells. This phenotype was accentuated in recall responses, which represent the chronic stimulation by autoantigens better than primary responses. This suggests that *Pbx1-d* expression contributes to lupus by promoting T_{FH} cells at the expense of iTreg differentiation, resulting in the production of class-switched affinity matured autoantibodies that are the hallmark of the *Sle1* susceptibility locus and lupus pathogenesis.

Lupus patients present high levels of circulating T_{FH}-like cells that correlate with disease activity (32, 33) and functional T_{FH} cells have been found in the kidneys of patients with lupus nephritis (34). T_{FH} cells are the limiting factor for GC size and function, and there is abundant evidence from several mouse models that unrestricted T_{FH} expansion leads to systemic autoimmunity (35, 36). Multiple studies have also found an association between decreased numbers or impaired function of Treg cells in lupus patients and mouse models (37). The differentiation of effector $CD4^+$ T cell subsets is a dynamic and plastic process, and cross-talks between the T_{FH} and Treg pathways have been described (30, 38). Although rapid progress has been made in recent years in mapping out the molecular pathways leading to Treg (39) and T_{FH} cell differentiation (40), many questions still remain, including the mechanisms by which the balance between these two subsets is maintained. We propose that PBX1 is involved in this process through its ability to regulate gene expression in a cell specific manner through complex interactions with its co-factors. The over-expression of dominant-negative *Pbx1-d* leads to an imbalance in T cell homeostasis: a modest *Pbx1-d* over-expression limits the spontaneous expansion or maintenance of the Treg subset in B6.*Sle1a1* mice, while a high over-expression of *Pbx1-d* expands T_{FH} cells *Pbx1-d* Tg mice. Homeostatic expansion in the context of BM chimera revealed a role for *Pbx1-d* Tg overexpression for Treg maintenance. Similarly, a recall response in a competitive setting

revealed a much stronger response of T_{FH} cells expressing *Pbx1-d* either as a transgene or endogenously. This could be due to a better survival of memory T_{FH} cells after the primary response, or to a better ability to respond to the challenge, two possibilities that we will explore in future experiments.

Interestingly, we found that the imbalance between Treg and T_{FH} cells was enhanced in the mLN. We have previously associated *Pbx1-d* expression with an impaired response to RA ((15) and this report), and the major effect of RA *in vivo* occurs in gut-associated lymphoid tissue. It is therefore possible that the anatomy of T_{FH} cell expansion in *Pbx1-d* Tg mice reflects the relative response to RA and commensal microbiota, an issue that will be explored in future studies. *Pbx1-d* led to T_{FH} cell expansion in spite of a relatively expanded T_{FR} subset, which is reminiscent of a recent study of mice with a specific deletion of PTEN in $Foxp3^+$ T cells, in which T_{FH} cell expansion occurred as a result of impaired Treg cell functions but in the presence of unchanged or expanded T_{FR} cell numbers (41). In addition to *Pbx1-d* expression level, other factors may contribute to the differences between B6.*Sle1a1* and *Pbx1-d* Tg mice. B6.*Sle1a1* mice express *Pbx1-d* in other cell types, such as mesenchymal stem cells, leading to an increased production of pro-inflammatory cytokines (21). Pbx1 also regulates the production of inflammatory cytokines in macrophages in response to apoptotic cells (42). Although we have shown that the *Sle1a1* T cell phenotypes are cell-intrinsic (15), we cannot rule out that *Pbx1-d* expression in other cell types may have additional modulatory effects on $CD4^+$ T cell differentiation

MicroRNAs are essential mediators of T_H cell plasticity, including the balance between Treg and T_{FH} cells (30). Numerous studies have documented different miRNA profiles in human and murine SLE (43–45), and causal relationships between overexpression of either miR-21 or miR-155 and lupus have been established (46, 47). We showed here that increased expression of miR-10a, miR-21 and miR-155 occurs in $CD4^+$ T cells before TC mice show autoimmune manifestations. Importantly, increased *Pbx1-d* expression in both the B6.*Sle1a1* congenic and *Pbx1-d* Tg $CD4^+$ T cells showed the same pattern of miRNA expression, implicating *Pbx1-d* as a primary driver regulating the intrinsic expression of these three miRNAs in T cells, either directly or indirectly. The existence of PBX1 binding sites in the distal promoter of each of these three miRNAs that are sufficient to increase transcription in the presence of Pbx1 supports this hypothesis. If Pbx1-d functions as a dominant negative transcription factor, it suggests that Pbx1-b is a negative regulator of these three miRNAs, especially for miR-10a and miR-155. Pbx1 can however bind to DNA indirectly through numerous co-factors (48, 49). Detailed studies will be necessary to unravel the molecular mechanisms by which Pbx1 isoforms regulate the expression of miR-10a, miR-21 and miR-155.

The exact role of each of these miRNAs in T cells overexpressing Pbx1-d could provide important cues on the mechanisms by which Pbx1 regulates T cell differentiation. miR-10a is over-expressed in B cells from lupus patients (44) and miR-10a stabilizes Treg cells (50) and prevents the conversion of pTreg into T_{FH} cells by targeting Bcl6 and its co-repressor Ncor2 in a TGF-β and RA-dependent manner (51). It was therefore unexpected to find consistently high levels of miR-10a expression in the $CD4^+$ T cells, including $Foxp3^+$ T cells, of the lupus congenic mice characterized here. Moreover, the level of miR-10a was

similar between *Pbx1-d* Tg and TC CD4$^+$ T cells, arguing that *Pbx1-d* overexpression is the main determinant of this dysregulation. miR-21 is elevated in lupus (52) and it regulates aberrant T cell responses by blocking PDCD4 expression (45). miR-21 expression has not been directly linked to either Treg or T_{FH} cells, but it is activated by STAT3 in T cells (53), and it is possible that its increased expression in *Pbx1-d* Tg CD4$^+$ T cells is secondary to their increased IL-21 expression. miR-155 is a central modulator of T cell functions (54). Receptor activation increases miR-155 expression in T cells, which regulates effector subset differentiation and maintenance. miR-155 deficiency has been associated with decreased T_H1 responses as well as low Treg cell numbers, which fits with *Pbx1-d* Tg expressing T cells showing high miR-155 expression, skewed T_H1 humoral responses and a reduced Treg population. Specific deletion of miR-155 in T cells showed an intrinsic requirement of miR-155 for T_{FH} cell differentiation (55). miR-155 deficiency normalized B cell functions and autoAb production in FAS-deficient mice (47). The role of miR-155 expression in T cells was however not addressed in this model. Our results demonstrate consistent high levels of miR-155 expression in the CD4$^+$ T cells of the lupus congenic mice examined in this study, including both Foxp3$^+$ and Foxp3$^-$ *Pbx1-d* Tg CD4$^+$ T cells. This is consistent with a model in which miR-155 favors T_{FH} over Treg cell differentiation and demonstrates that *Pbx1-d* overexpression is sufficient to drive this process. Interestingly, we found an overexpression of the miR-17~92 cluster in *Sle1a1* Treg cells but no difference in *Pbx1-d* Tg Treg cells, or in non-Treg cells in either strain. miR-17~92 prevents pTreg cell differentiation (56), which fits with our findings that Treg cells are more affected in *Sle1a1* than *Pbx1-d* Tg T cells. Moreover, miR-17~92 over-expression in lymphocytes leads to autoimmune phenotypes in mice (57), suggesting that it may be a mechanism by which *Pbx1-d* overexpression contributes to autoimmunity.

In conclusion, the phenotypes and CD4$^+$ T cell differentiation in *Pbx1-d* Tg mice are similar to that of B6.*Sle1a1* mice, which establishes *Pbx1* as the gene responsible for the *Sle1a1* phenotype. It also highlights critical roles for the lupus development in regulating Treg and T_{FH} cell differentiation, and developing humoral autoimmunity. The *Pbx1-d* Tg mice provide a novel model to investigate T cell intrinsic mechanisms that regulate Treg/T_{FH} homeostasis. Further studies are required to identify the *Pbx1/Pbx1-d*-regulated genes in T cells and their contribution to CD4$^+$ T cell differentiation and effector functions.

Supplementary Material

Refer to Web version on PubMed Central for supplementary material.

Acknowledgments

We are indebted to Dr. Edward Chan for his advice on miRNAs. We thank Leilani Zeumer, Nathalie Kanda, Shun Lu, and Yuxin Niu for outstanding technical help.

Abbreviations

Ab antibody

Ag antigen

ANA	anti-nuclear Ab
B6	C57BL/6J mice
B6.Ly5^{a}	B6.SJL-*Ptprc*^{a}*Pep3*^{b}/BoyJ
BM	bone marrow
GC	germinal center
iTreg	induced Treg
mLN	mesenteric lymph node
OVA	ovalbumin
pTreg	peripheral Treg
SLE	systemic lupus erythematosus
TC	B6.NZM-*Sle1*$^{NZM2410/Aeg}$*Sle2*$^{NZM2410/Aeg}$*Sle3*$^{NZM2410/Aeg}$/LmoJ
TD	T-dependent
Teff	effector T cells
Tg	transgene
T_{EM}	$CD44^{+}CD62L^{-}CD4^{+}$ effector memory T cells
T_{FH}	$CXCR5^{+}PD\text{-}1^{+}BCL6^{+}FOXP3^{-}CD4^{+}$ follicular helper T cells
T_{FR}	$CD4^{+}PD1^{+}CXCR5^{+}Bcl6^{+}Foxp3^{+}$ follicular regulatory T cells
T_{N}	$CD44^{-}CD62L^{+}$ naïve T cells
Treg	regulatory T cells
tTreg	thymic Treg

References

1. Morel L, Rudofsky UH, Longmate JA, Schiffenbauer J, Wakeland EK. Polygenic control of susceptibility to murine systemic lupus erythematosus. Immunity. 1994; 1:219–229. [PubMed: 7889410]
2. Morel L, Yu Y, Blenman KR, Caldwell RA, Wakeland EK. Production of congenic mouse strains carrying genomic intervals containing SLE-susceptibility genes derived from the SLE-prone NZM2410 strain. Mammalian genome. 1996; 7:335–339. [PubMed: 8661718]
3. Morel L. Mapping lupus susceptibility genes in the NZM2410 mouse model. Adv Immunol. 2012; 115:113–139. [PubMed: 22608257]
4. Morel L, Tian XH, Croker BP, Wakeland EK. Epistatic modifiers of autoimmunity in a murine model of lupus nephritis. Immunity. 1999; 11:131–139. [PubMed: 10485648]
5. Morel L, Croker BP, Blenman KR, Mohan C, Huang G, Gilkeson G, Wakeland EK. Genetic reconstitution of systemic lupus erythematosus immunopathology with polycongenic murine strains. Proc Natl Acad Sci USA. 2000; 97:6670–6675. [PubMed: 10841565]

6. Mohan C, Alas E, Morel L, Yang P, Wakeland EK. Genetic dissection of SLE pathogenesis. Sle1 on murine chromosome 1 leads to a selective loss of tolerance to H2A/H2B/DNA subnucleosomes. J Clin Invest. 1998; 101:1362–1372. [PubMed: 9502778]
7. Sobel ES, Satoh M, Chen WF, Wakeland EK, Morel L. The major murine systemic lupus erythematosus susceptibility locus Sle1 results in abnormal functions of both B and T cells. J Immunol. 2002; 169:2694–2700. [PubMed: 12193743]
8. Morel L, Blenman KR, Croker BP, Wakeland EK. The major murine systemic lupus erythematosus susceptibility locus, Sle1, is a cluster of functionally related genes. Proc Natl Acad Sci USA. 2001; 98:1787–1792. [PubMed: 11172029]
9. Cuda CM, Wan S, Sobel ES, Croker BP, Morel L. Murine lupus susceptibility locus Sle1a controls regulatory T cell number and function through multiple mechanisms. J Immunol. 2007; 179:7439–7447. [PubMed: 18025188]
10. Chen Y, Perry D, Boackle SA, Sobel ES, Molina H, Croker BP, Morel L. Several genes contribute to the production of autoreactive B and T cells in the murine lupus susceptibility locus Sle1c. J Immunol. 2005; 175:1080–1089. [PubMed: 16002709]
11. Chen Y, Cuda C, Morel L. Genetic determination of T cell help in loss of tolerance to nuclear antigens. J Immunol. 2005; 174:7692–7702. [PubMed: 15944270]
12. Wandstrat AE, Nguyen C, Limaye N, Chan AY, Subramanian S, Tian XH, Yim YS, Pertsemlidis A, Garner HR Jr, Morel L, Wakeland EK. Association of extensive polymorphisms in the SLAM/CD2 gene cluster with murine lupus. Immunity. 2004; 21:769–780. [PubMed: 15589166]
13. Keszei M, Detre C, Rietdijk ST, Munoz P, Romero X, Berger SB, Calpe S, Liao G, Castro W, Julien A, Wu YY, Shin DM, Sancho J, Zubiaur M, Morse HC III, Morel L, Engel P, Wang N, Terhorst C. A novel isoform of the Ly108 gene ameliorates murine lupus. J Exp Med. 2011; 208:811–822. [PubMed: 21422172]
14. Cuda CM, Zeumer L, Sobel ES, Croker BP, Morel L. Murine lupus susceptibility locus Sle1a requires the expression of two sub-loci to induce inflammatory T cells. Genes and immunity. 2010; 11:542–553. [PubMed: 20445563]
15. Cuda CM, Li S, Liang S, Yin Y, Potula HH, Xu Z, Sengupta M, Chen Y, Butfiloski E, Baker H, Chang LJ, Dozmorov I, Sobel ES, Morel L. Pre-B cell leukemia homeobox 1 is associated with lupus susceptibility in mice and humans. J Immunol. 2012; 188:604–614. [PubMed: 22180614]
16. Sagerstrom CG. PbX marks the spot. Dev Cell. 2004; 6:737–738. [PubMed: 15177017]
17. Laurent A, Bihan R, Omilli F, Deschamps S, Pellerin I. PBX proteins: much more than Hox cofactors. Intl J Dev Biol. 2008; 52:9–20.
18. Sengupta M, Liang S, Potula HHS, Chang LJ, Morel L. The SLE-associated Pbx1-d isoform acts as a dominant-negative transcriptional regulator. Genes and Immunity. 2012; 13:653–657. [PubMed: 22992721]
19. Sobel ES, Brusko TM, Butfiloski EJ, Hou W, Li S, Cuda CM, Abid AN, Reeves WH, Morel L. Defective response of CD4+ T cells to retinoic acid and TGFbeta in systemic lupus erythematosus. Arthritis Res Ther. 2011; 13:R106. [PubMed: 21708033]
20. Sanyal M, Tung JW, Karsunky H, Zeng H, Selleri L, Weissman IL, Herzenberg LA, Cleary ML. B-cell development fails in the absence of the Pbx1 proto-oncogene. Blood. 2007; 109:4191–4199. [PubMed: 17244677]
21. Lu S, Zeumer L, Sorensen H, Yang H, Ng Y, Yu F, Riva A, Croker B, Wallet S, Morel L. The murine Pbx1-d lupus susceptibility allele accelerates mesenchymal stem cell differentiation and impairs their immunosuppressive function. J Immunol. 2015; 194:43–55. [PubMed: 25416808]
22. Bettelli E, Carrier Y, Gao W, Korn T, Strom TB, Oukka M, Weiner HL, Kuchroo VK. Reciprocal developmental pathways for the generation of pathogenic effector TH17 and regulatory T cells. Nature. 2006; 441:235–238. [PubMed: 16648838]
23. Yin Y, Choi SC, Xu Z, Perry DJ, Seay H, Croker BP, Sobel ES, Brusko TM, Morel L. Normalization of CD4+ T cell metabolism reverses lupus. Sci Transl Med. 2015; 7:274ra218.
24. Vogelzang A, McGuire HM, Yu D, Sprent J, Mackay CR, King C. A fundamental role for interleukin-21 in the generation of T follicular helper cells. Immunity. 2008; 29:127–137. [PubMed: 18602282]

25. Spolski R, Leonard WJ. Interleukin-21: a double-edged sword with therapeutic potential. Nat Rev Drug Disc. 2014; 13:379–395.
26. Ozaki K, Spolski R, Ettinger R, Kim HP, Wang G, Qi CF, Hwu P, Shaffer DJ, Akilesh S, Roopenian DC, Morse HC 3rd, Lipsky PE, Leonard WJ. Regulation of B cell differentiation and plasma cell generation by IL-21, a novel inducer of Blimp-1 and Bcl-6. J Immunol. 2004; 173:5361–5371. [PubMed: 15494482]
27. Luthje K, Kallies A, Shimohakamada Y, Belz GT, Light A, Tarlinton DM, Nutt SL. The development and fate of follicular helper T cells defined by an IL-21 reporter mouse. Nat Immunol. 2012; 13:491–498. [PubMed: 22466669]
28. Barnden MJ, Allison J, Heath WR, Carbone FR. Defective TCR expression in transgenic mice constructed using cDNA-based alpha- and beta-chain genes under the control of heterologous regulatory elements. Immunol Cell Biol. 1998; 76:34–40. [PubMed: 9553774]
29. Odegard JM, Marks BR, DiPlacido LD, Poholek AC, Kono DH, Dong C, Flavell RA, Craft J. ICOS-dependent extrafollicular helper T cells elicit IgG production via IL-21 in systemic autoimmunity. J Exp Med. 2008; 205:2873–2886. [PubMed: 18981236]
30. Baumjohann D, Ansel KM. MicroRNA-mediated regulation of T helper cell differentiation and plasticity. Nat Rev Immunol. 2013; 13:666–678. [PubMed: 23907446]
31. Velu CS, Chaubey A, Phelan JD, Horman SR, Wunderlich M, Guzman ML, Jegga AG, Zeleznik-Le NJ, Chen J, Mulloy JC, Cancelas JA, Jordan CT, Aronow BJ, Marcucci G, Bhat B, Gebelein B, Grimes HL. Therapeutic antagonists of microRNAs deplete leukemia-initiating cell activity. J Clin Invest. 2014; 124:222–236. [PubMed: 24334453]
32. Choi J-Y, Hsi-enHo J, Pasoto SG, Bunin V, Kim S, Carrasco S, Borba EF, Gonçalves CR, Costa PR, Kallas EG, Bonfa E, Craft J. Circulating follicular helper-like T cells in systemic lupus erythematosus: Association with disease activity. Arth Rheumatol. 2015; 4:988–999. [PubMed: 25581113]
33. Wang L, Zhao P, Ma L, Shan Y, Jiang Z, Wang J, Jiang Y. Increased interleukin 21 and follicular helper T-like cells and reduced interleukin 10+ B cells in patients with new-onset systemic lupus erythematosus. J Rheumatol. 2014; 41:1781–1792. [PubMed: 25028374]
34. Liarski VM, Kaverina N, Chang A, Brandt D, Yanez D, Talasnik L, Carlesso G, Herbst R, Utset TO, Labno C, Peng Y, Jiang Y, Giger ML, Clark MR. Cell distance mapping identifies functional T follicular helper cells in inflamed human renal tissue. Sci Transl Med. 2014; 6:230ra246.
35. Craft JE. Follicular helper T cells in immunity and systemic autoimmunity. Nat Rev Rheumatol. 2012; 8:337–347. [PubMed: 22549246]
36. Pratama A, Vinuesa CG. Control of TFH cell numbers: why and how? Immunol Cell Biol. 2014; 92:40–48. [PubMed: 24189162]
37. Ohl K, Tenbrock K. Regulatory T cells in systemic lupus erythematosus. Europ J Immunol. 2015; 45:344–355.
38. Tsuji M, Komatsu N, Kawamoto S, Suzuki K, Kanagawa O, Honjo T, Hori S, Fagarasan S. Preferential generation of follicular B helper T cells from Foxp3+ T cells in gut Peyer's patches. Science. 2009; 323:1488–1492. [PubMed: 19286559]
39. Ohkura N, Kitagawa Y, Sakaguchi S. Development and maintenance of regulatory T cells. Immunity. 2013; 38:414–423. [PubMed: 23521883]
40. Crotty S. T follicular helper cell differentiation, function, and roles in disease. Immunity. 2014; 41:529–542. [PubMed: 25367570]
41. Shrestha S, Yang K, Guy C, Vogel P, Neale G, Chi H. Treg cells require the phosphatase PTEN to restrain TH1 and TFH cell responses. Nat Immunol. 2015; 16:178–187. [PubMed: 25559258]
42. Chung EY, Liu J, Homma Y, Zhang Y, Brendolan A, Saggese M, Han J, Silverstein R, Selleri L, Ma X. Interleukin-10 expression in macrophages during phagocytosis of apoptotic cells is mediated by homeodomain proteins Pbx1 and Prep-1. Immunity. 2007; 27:952–964. [PubMed: 18093541]
43. Dai Y, Huang YS, Tang M, Lv TY, Hu CX, Tan YH, Xu ZM, Yin YB. Microarray analysis of microRNA expression in peripheral blood cells of systemic lupus erythematosus patients. Lupus. 2007; 16:939–946. [PubMed: 18042587]

44. Martinez-Ramos R, Garcia-Lozano JR, Lucena JM, Castillo-Palma MJ, Garcia-Hernandez F, Rodriguez MC, Nunez-Roldan A, Gonzalez-Escribano MF. Differential expression pattern of microRNAs in CD4+ and CD19+ cells from asymptomatic patients with systemic lupus erythematosus. Lupus. 2014; 23:353–359. [PubMed: 24509687]
45. Stagakis E, Bertsias G, Verginis P, Nakou M, Hatziapostolou M, Kritikos H, Iliopoulos D, Boumpas DT. Identification of novel microRNA signatures linked to human lupus disease activity and pathogenesis: miR-21 regulates aberrant T cell responses through regulation of PDCD4 expression. Ann Rheum Dis. 2011; 70:1496–1506. [PubMed: 21602271]
46. Pan W, Zhu S, Yuan M, Cui H, Wang L, Luo X, Li J, Zhou H, Tang Y, Shen N. MicroRNA-21 and microRNA-148a contribute to DNA hypomethylation in lupus CD4+ T cells by directly and indirectly targeting DNA methyltransferase 1. J Immunol. 2010; 184:6773–6781. [PubMed: 20483747]
47. Thai TH, Patterson HC, Pham DH, Kis-Toth K, Kaminski DA, Tsokos GC. Deletion of microRNA-155 reduces autoantibody responses and alleviates lupus-like disease in the Fas(lpr) mouse. Proc Natl Acad Sci USA. 2013; 110:20194–20199. [PubMed: 24282294]
48. Bjerke GA, Hyman-Walsh C, Wotton D. Cooperative transcriptional activation by Klf4, Meis2, and Pbx1. Mol Cell Biol. 2011; 31:3723–3733. [PubMed: 21746878]
49. Penkov D, Mateos San Martin D, Fernandez-Diaz LC, Rossello CA, Torroja C, Sanchez-Cabo F, Warnatz HJ, Sultan M, Yaspo ML, Gabrieli A, Tkachuk V, Brendolan A, Blasi F, Torres M. Analysis of the DNA-binding profile and function of TALE homeoproteins reveals their specialization and specific interactions with Hox genes/proteins. Cell Rep. 2013; 3:1321–1333. [PubMed: 23602564]
50. Jeker LT, Zhou X, Gershberg K, de Kouchkovsky D, Morar MM, Stadthagen G, Lund AH, Bluestone JA. MicroRNA 10a Marks Regulatory T Cells. PLoS ONE. 2012; 7:e36684. [PubMed: 22629323]
51. Takahashi H, Kanno T, Nakayamada S, Hirahara K, Sciume G, Muljo SA, Kuchen S, Casellas R, Wei L, Kanno Y, O'Shea JJ. TGF-beta and retinoic acid induce the microRNA miR-10a, which targets Bcl-6 and constrains the plasticity of helper T cells. Nat Immunol. 2012; 13:587–595. [PubMed: 22544395]
52. Pan W, Zhu S, Yuan M, Cui H, Wang L, Luo X, Li J, Zhou H, Tang Y, Shen N. MicroRNA-21 and MicroRNA-148a Contribute to DNA Hypomethylation in Lupus CD4+ T Cells by Directly and Indirectly Targeting DNA Methyltransferase 1. J Immunol. 2010; 184:6773–6781. [PubMed: 20483747]
53. Sawant DV, Wu H, Kaplan MH, Dent AL. The Bcl6 target gene microRNA-21 promotes Th2 differentiation by a T cell intrinsic pathway. Mol Immunol. 2013; 54:435–442. [PubMed: 23416424]
54. Lind EF, Ohashi PS. Mir-155, a central modulator of T-cell responses. Eu J Immunol. 2014; 44:11–15.
55. Hu R, Kagele DA, Huffaker TB, Runtsch MC, Alexander M, Liu J, Bake E, Su W, Williams MA, Rao DS, Moller T, Garden GA, Round JL, O'Connell RM. miR-155 promotes T follicular helper cell accumulation during chronic, low-grade inflammation. Immunity. 2014; 41:605–619. [PubMed: 25367574]
56. Jiang S, Li C, Olive V, Lykken E, Feng F, Sevilla J, Wan Y, He L, Li QJ. Molecular dissection of the miR-17-92 cluster's critical dual roles in promoting Th1 responses and preventing inducible Treg differentiation. Blood. 2011; 118:5487–97. [PubMed: 21972292]
57. Xiao S, Jin H, Korn T, Liu SM, Oukka M, Lim B, Kuchroo VK. Retinoic acid increases Foxp3+ regulatory T cells and inhibits development of Th17 cells by enhancing TGF-β-driven Smad3 signaling and inhibiting IL-6 and IL-23 receptor expression. J Immunol. 2008; 181:2277–2284. [PubMed: 18684916]

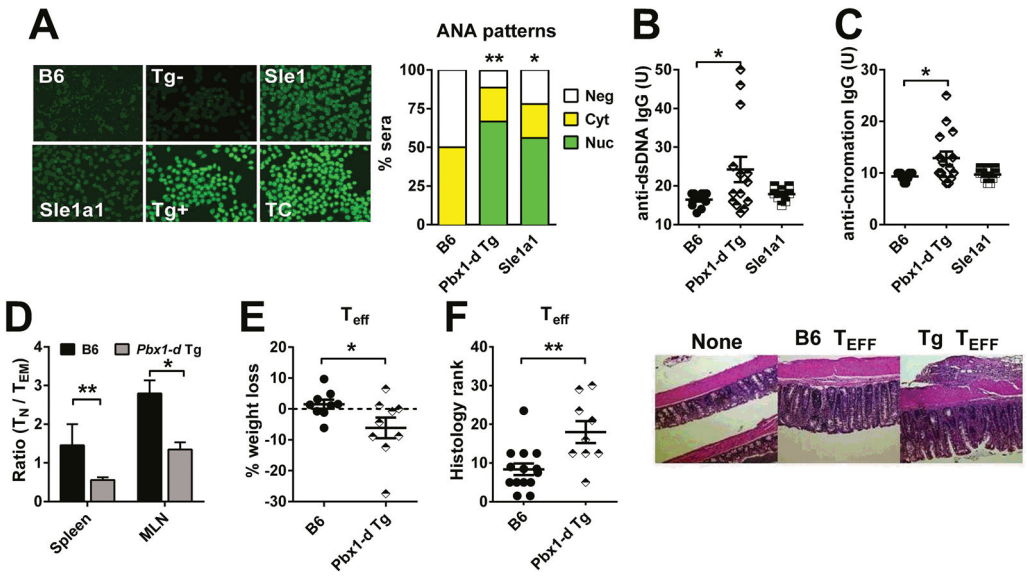

Figure 1. Pbx1-d overexpression in CD4$^+$ T cells reproduced the phenotypes of B6.Sle1a1 mice

A. Representative serum ANA staining patterns in B6, *Pbx1-d* Tg$^-$ (Tg$^-$), B6.*Sle1*, B6.*Sle1a1*, *Pbx1-d* Tg (Tg$^+$), and TC mice as positive control. The pattern distribution (nuclear, cytoplasmic or negative) was significantly different between *Pbx1-d* Tg$^+$ or B6.*Sle1a1* and (B6 + Tg$^-$) combined mice (n = 10–18 per strain). Serum anti-dsDNA (**B**) and anti-chromatin (**C**) IgG (n = 10–15). **D**. T_N/T_{EM} ratio in the spleen and mLN from B6 and *Pbx1-d* Tg mice (n = 3–4). Mice were 7–12 month old for A–D. **E**. Maximum weekly percentage of body weight loss by B6.*Rag1*$^{-/-}$ mice up to 8 weeks after transfer of *Pbx1-d* Tg or B6 T_{Eff} cells. **F.** Colitis pathology score 8 weeks after transfer with representative images of colon histology taken with the same 40X magnification shown on the right. Each symbol represents a mouse. *$P < 0.05$, **$P < 0.01$.

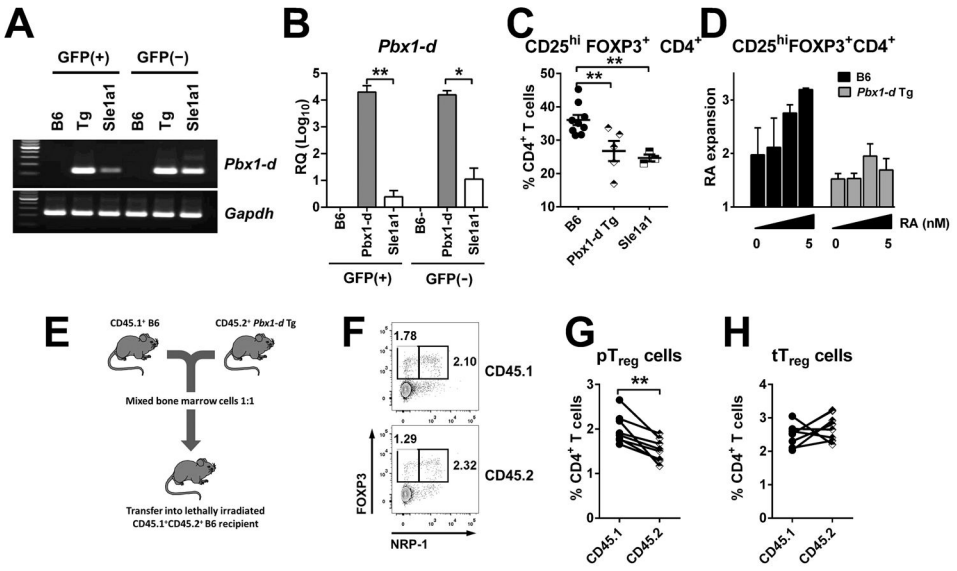

Figure 2. *Pbx1-d* overexpression impaired pTreg cell induction

bx1-d mRNA expression in Foxp3$^+$ and Foxp3$^-$CD4$^+$ T cells purified from B6.*Foxp3*^{egfp}, *Pbx1-d* Tg.*Foxp3*^{egfp}, and B6.*Sle1a1.Foxp3*^{egfp} mice analyzed by conventional (**A**) and quantitative (**B**) RT-PCR with the data presented relative to B6 (RQ; n = 3). **C**. Frequency of Foxp3$^+$ Treg cells in the mLN of 10–12 month-old B6, *Pbx1-d* Tg, and B6.*Sle1a1* mice. Each symbol represents a mouse. **D**. Foxp3 induction in CD4$^+$CD25$^-$T cells in the presence of TGF-β, presented as the ratio of induction with over without RA. **E–H**. Mixed-BM chimera analysis of Treg cells. **E**. Experimental design. **F**. Gates for Foxp3$^+$Nrp-1$^+$ tTreg and Foxp3$^+$Nrp-1$^-$pTreg cells within the total CD4$^+$CD8$^-$CD45.1$^+$ or CD45.2$^+$ thymocytes. Percentage of pTreg (**G**) and tTreg cells (**H**) in the chimeras with each linked symbol representing a mouse. *$P < 0.05$, ** $P < 0.01$.

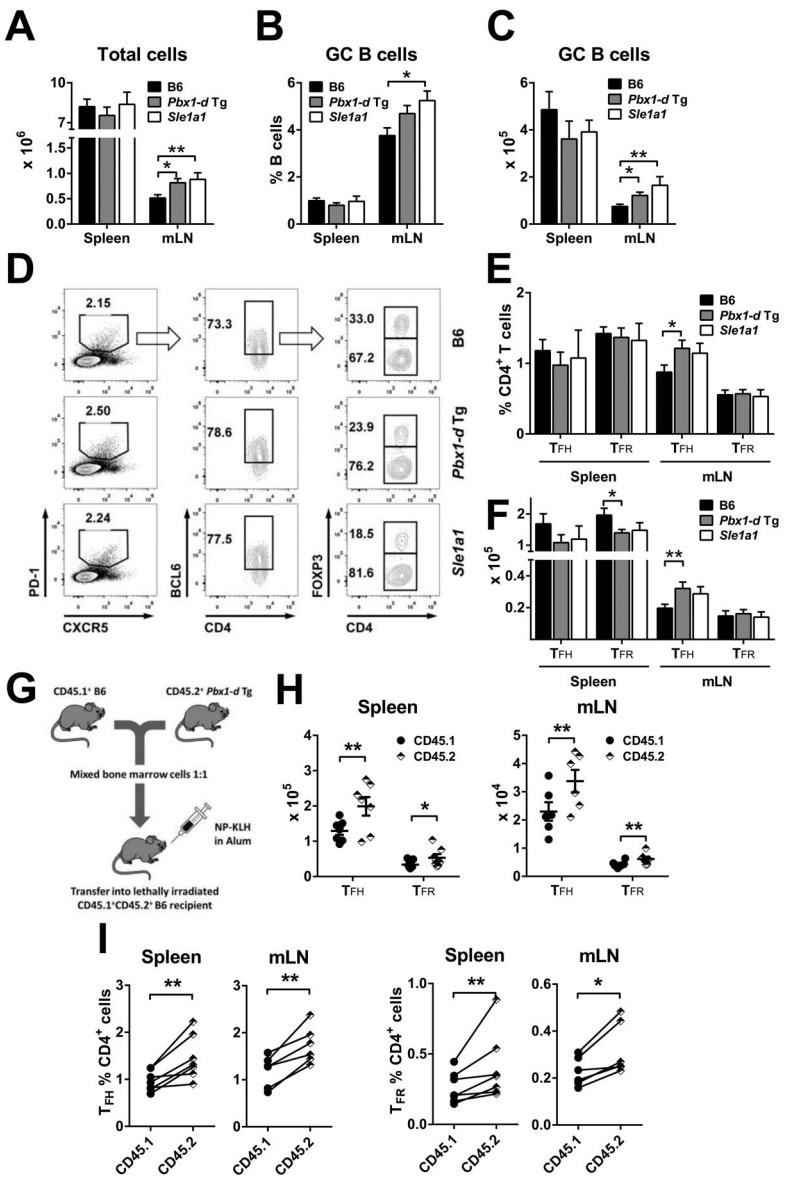

Figure 3. *Pbx1-d* Tg expression in CD4$^+$ T cells expanded GC lymphocytes

Absolute numbers of lymphocytes (**A**), percentages (**B**) and absolute numbers (**C**) of B220$^+$GL-7$^+$FAS$^+$ GC B cells in the spleen and mLN from 2 month-old B6, *Pbx1-d* Tg, and B6.*Sle1a1* mice. **D**. Representative FACS plots for CD4$^+$CXCR5$^+$PD-1$^+$Bcl6$^+$Foxp3$^+$ T_{FR} and CD4$^+$CXCR5$^+$PD-1 $^+$Bcl6$^+$Foxp3$^-$$T_{FH}$ cells. Percentages (**E**) and absolute numbers (**F**) of T_{FH} and T_{FR} cells. n = 5–10. **G–I**: Follicular T cell expansion in response to NP-KLH immunization in mixed BM chimeras. **G**: Experimental strategy. Absolute numbers (**H**) and percentages (**I**) of T_{FH} and T_{FR} cells 7 d after immunization gated according to their strain of origin: CD45.1: B6, CD45.2: *Pbx1-d* Tg. Each symbol (linked in **I**) represents a mouse. *$P < 0.05$, **$P < 0.01$.

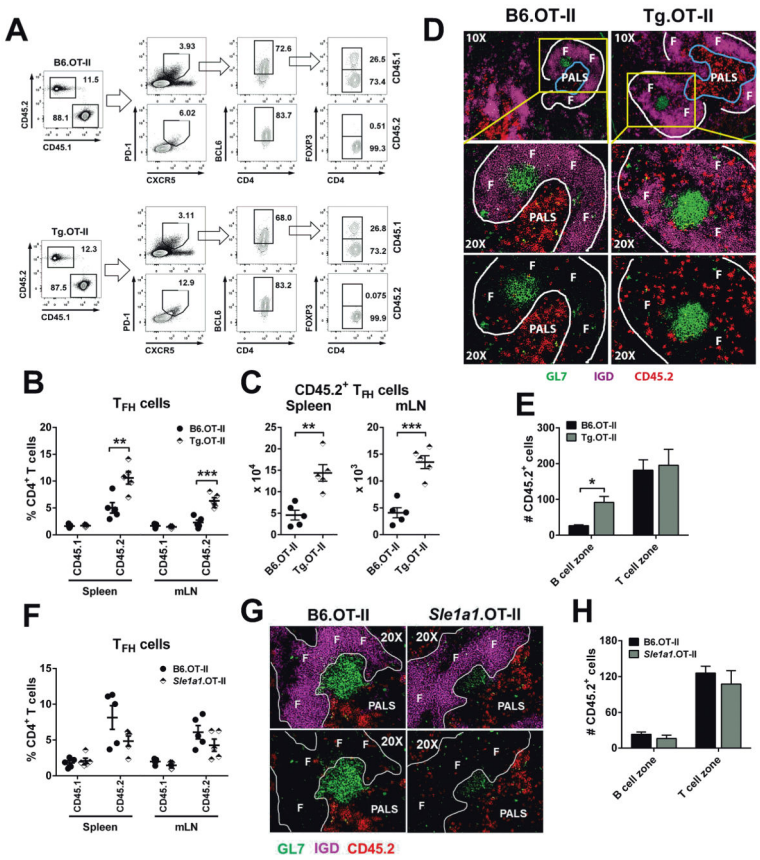

Figure 4. *Pbx1-d* Tg expression in CD4$^+$ T cells regulated Ag-specific T_{FH} cell differentiation

T_{FH} cells were analyzed 5 d after NP-OVA immunization of CD45.1$^+$ B6 mice transferred with CD45.2$^+$ naïve B6.OT-II or *Pbx1-d* Tg.OT-II cells. **A**. Representative flow cytometric plots showing mLN CD4$^+$ CD45.1$^+$ (endogenous) and CD45.2$^+$ (transferred) gated CXCR5$^+$PD-1$^+$ T_{FH} and T_{FR} cells. **B**. Percentages of donor and recipient T_{FH} cells. **C**. Absolute numbers of donor T_{FH} cells. Each symbol represents a recipient mouse. **D**. Localization of donor OT-II CD4$^+$ T cells (CD45.2$^+$, red) relative to B cell follicles (IgD$^+$, F), GCs (GL7$^+$, green), and periarteriolar lymphoid sheaths (PALS). The framed areas in the 10x magnification are shown below at 20x, with the bottom panels showing only the outline of the IgG$^+$ B cell follicles for a better comparison of the number and location of CD45.2$^+$ T cells. **E**. Numbers of B6.OT-II or *Pbx1-d* Tg.OT-II CD4$^+$ T cells in B or T cell zones, showing mean ± SEM from 3–7 GC regions per mouse from 3 mice per strain. **F**. Percentages of donor and recipient T_{FH} cells 5 d after NP-OVA immunization of CD45.1$^+$ B6 mice transferred with CD45.2$^+$ naïve B6.OT-II or *Sle1a1*.OT-II cells. **G**. Representative 20x spleen sections of B6.OT-II or *Sle1a1*.OT-II cell recipients, as in **D. H**. Numbers of B6.OT-II or *Sle1a1*.OT-II CD4$^+$ T cells in B or T cell zones, showing mean ± SEM from 3–7 GC regions per mouse from 5 mice per strain. *$P < 0.05$, **$P < 0.01$.

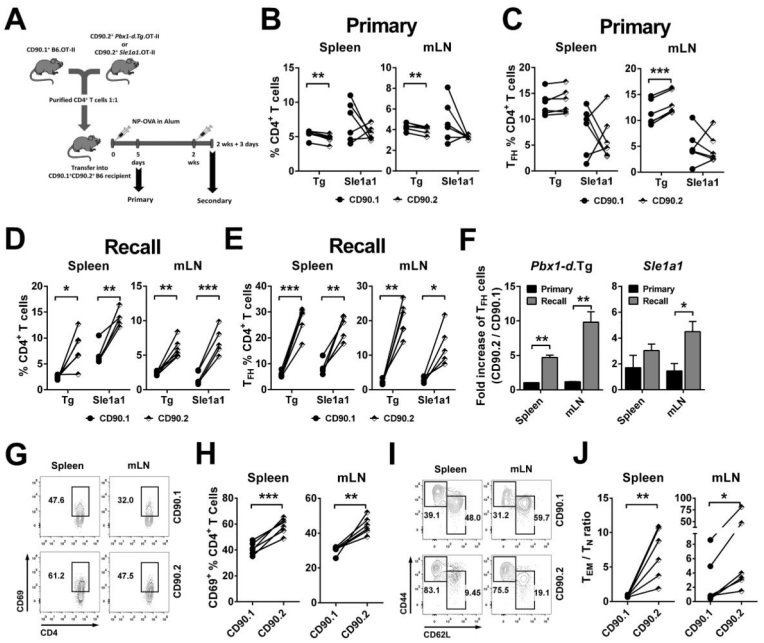

Figure 5. *Pbx1-d* intrinsically regulated T_{FH} cell differentiation and amplified recall responses

A. Experimental design for primary and recall response after mixed adoptive transfer of CD90.1$^+$ B6.OT-II and CD90.2$^+$ *Pbx1-d* Tg.OT-II or *Sle1a1*.OT-II CD4$^+$ T cells into (B6 x B6.*Thy1*^{a})F1 mice. Percentages of CD90.1$^+$ B6.OT-II and CD90.2$^+$ *Pbx1-d* Tg.OT-II or *Sle1a1*.OT-II CD4$^+$ T cells (**B** and **D**) and T_{FH} cells (**C** and **E**) from each genotype in the primary (**B** and **C**) and recall (**D** and **E**) responses. **F**. Fold increase of T_{FH} cells in recall vs. primary response, calculated as the ratio of CD90.2$^+$ /CD90.1$^+$ T_{FH} cells. Representative flow cytometric plots and corresponding percentages of CD4$^+$CD69$^+$ activated T (**G** and **H**) and T_{EM} / T_N CD4$^+$ T cells ratios (**I** and **J**) in CD90.1$^+$ B6.OT-II and CD90.2$^+$ *Pbx1-d*.OT-II Tg donor cells in the recall response. Each linked symbol represents a recipient mouse. n = 5–6, $*P < 0.05$, $**P < 0.01$, $***P < 0.001$.

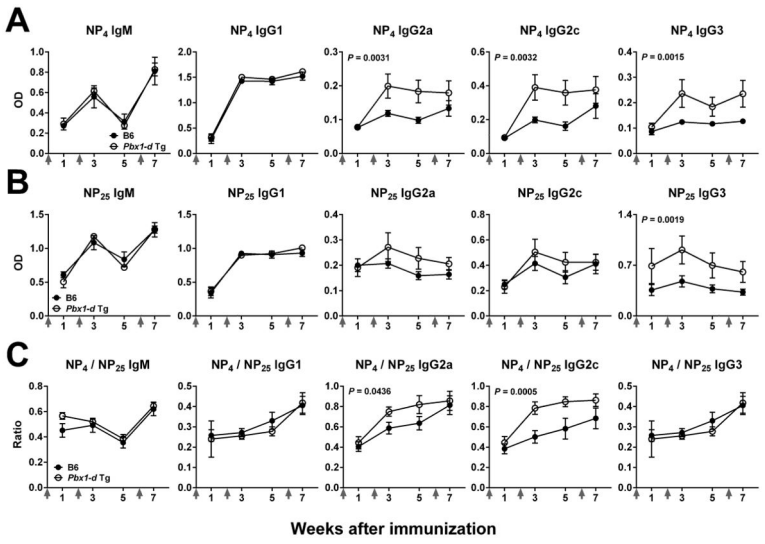

Figure 6. *Pbx1-d* Tg expression in CD4$^+$ T cells increased affinity maturation of T_H1-related isotypes

B6 and *Pbx1-d* Tg mice were immunized with NP-KLH then boosted 2 and 6 weeks later (arrows on X axes). Serum levels of NP-specific Abs 1 wk before and after boosting measured in plates coated with NP_4 (**A**) or NP_{25} (**B**) BSA. **C**. Affinity measured as the NP_4 / NP_{25} ratio for each isotype, n = 5.

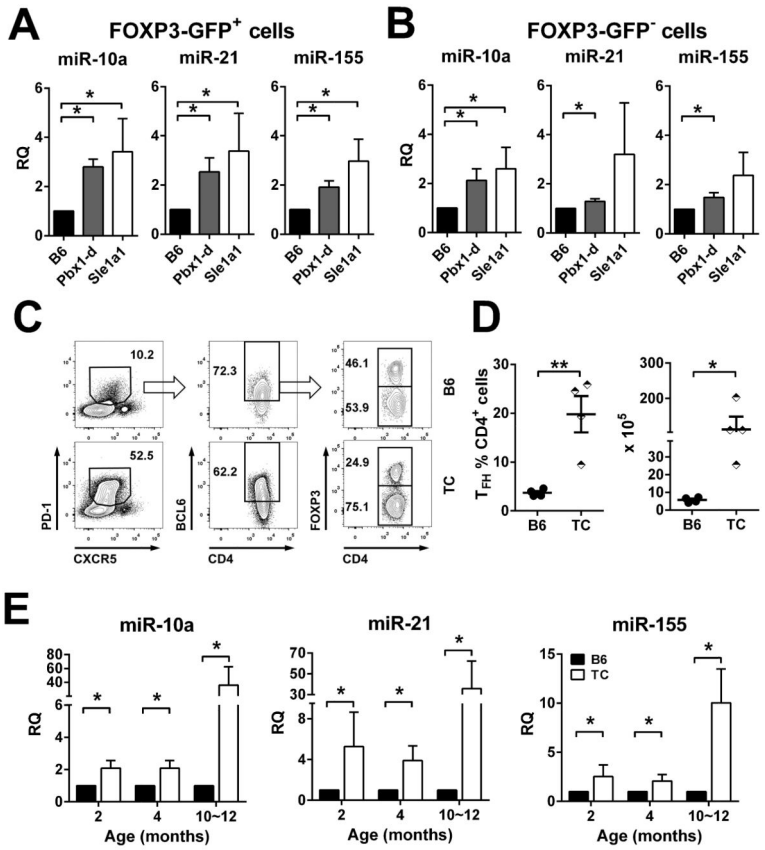

Figure 7. *Pbx1-d* Tg in CD4$^+$ T cells increased the expression of miR-10a, miR-21, and miR-155

miRNA expression was analyzed by qPCR in FOXP3$^+$-GFP$^+$ (**A**) and FOXP3-GFP$^-$ (**B**) CD4$^+$ T cells from *Pbx1-d* Tg.*Foxp3*^{egfp}, B6.*Sle1a1.Foxp3*^{egfp}, and B6.*Foxp3*^{egfp} spleens. Representative FACS plots for follicular T cells in spleens from 4 month old B6 and TC mice (**C**) and corresponding percentages and absolute numbers of T_{FH} cells (**D**). **E**. miRNAs expression in CD4$^+$ T cells from B6 and TC mice at 2, 4, and 10–12 month of age, n = 3–4.

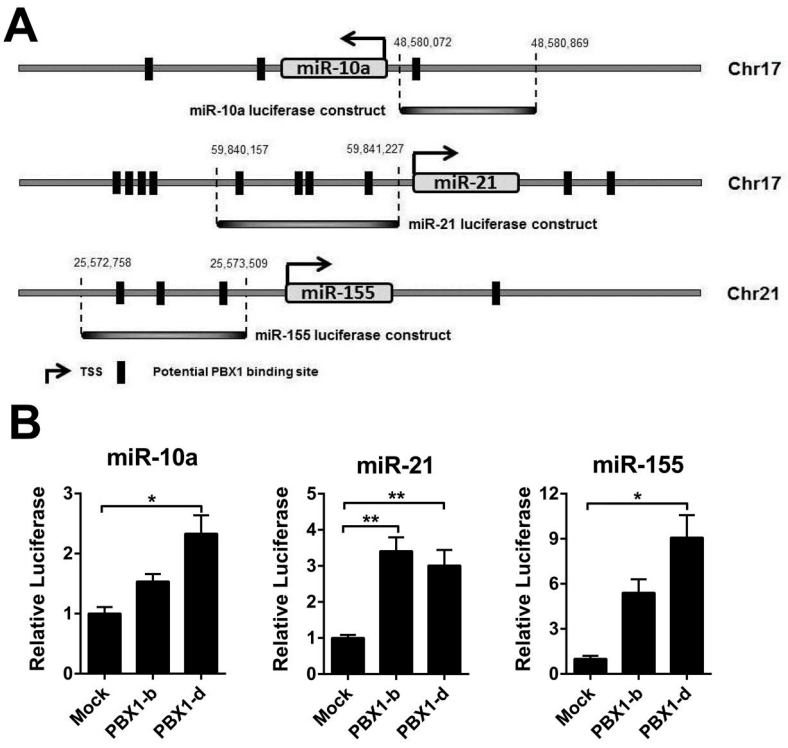

Figure 8. Human PBX1 binds to the promoter of miR-10a, miR-21, and miR-155

A. miRNA luciferase constructs containing predicted PBX1 binding sites were selected using Jaspar3. The regions used in the luciferase assays are indicated for each locus. **B**. Dual luciferase analyses of miR-10a, miR-21 and miR-155 expression in the presence of either PBX1-b or PBX1-d, showing fold change relative to the absence of PBX1 expression plasmid. All results are expressed as mean ± SD from at least three independent experiments.